Journal of Computational Neuroscience 12, 39–53, 2002

A Spiking Neuron Model for Binocular Rivalry

CARLO R. LAING
Department of Mathematics, University of Pittsburgh, Pittsburgh, PA 15260, USA; Department of Physics, University of Ottawa, 150 Louis Pasteur, Ottawa, Ontario, Canada K1N 6N5
claing@science.uottawa.ca

CARSON C. CHOW
Department of Mathematics, University of Pittsburgh, Pittsburgh, PA 15260, USA
ccc@math.pitt.edu

Received November 27, 2000; Revised October 26, 2001; Accepted November 29, 2001

Action Editor: Kenneth D. Miller

Abstract. We present a biologically plausible model of binocular rivalry consisting of a network of Hodgkin-Huxley type neurons. Our model accounts for the experimentally and psychophysically observed phenomena: (1) it reproduces the distribution of dominance durations seen in both humans and primates, (2) it exhibits a lack of correlation between lengths of successive dominance durations, (3) variation of stimulus strength to one eye influences only the mean dominance duration of the contralateral eye, not the mean dominance duration of the ipsilateral eye, (4) increasing both stimuli strengths in parallel decreases the mean dominance durations. We have also derived a reduced population rate model from our spiking model from which explicit expressions for the dependence of the dominance durations on input strengths are analytically calculated. We also use this reduced model to derive an expression for the distribution of dominance durations seen within an individual.

Keywords: binocular rivalry, multistable perception, visual perception

1. Introduction

Binocular rivalry occurs when the two eyes are presented with drastically different images. Only one of the images is perceived at a given time, and every few seconds there is alternation between the perceived images. The perceived durations of the images are stochastic and uncorrelated with previous perceived durations (Fox and Herrmann, 1967; Walker, 1975). Also, changing the contrast of the images will change the dominance durations of the perceptions in specific ways.

It is not yet clear exactly what is rivaling during binocular rivalry (Lee and Blake, 1999; Logothetis et al., 1996). It was traditionally thought that the rivalry was between the two eyes (Blake, 1989; Lehky, 1988). However, there is more recent evidence that the neurons at the site(s) of rivalry have access to information from both eyes (Carlson and He, 2000; Kovacs et al., 1996; Lumer et al., 1998; Ngo et al., 2000), and these experimental results cannot be explained in terms of "eye rivalry" (although see Lee and Blake, 1999, for an indication of how changing stimulus characteristics can produce either "eye rivalry" or "stimulus rivalry").

Recordings in the cortex of monkeys undergoing binocular rivalry indicate that the neuronal activity of binocular rather than monocular neurons is correlated with the perception of one of the presented images (Leopold and Logothetis, 1996, 1999; Logothetis, 1998; Logothetis et al., 1996; Logothetis

and Schall, 1989). The proportion of neurons that are active only when one of the images is perceived increases as one moves up the visual pathway (Leopold and Logothetis, 1999; Logothetis, 1998). It should be noted that while some neurons are more active when their preferred image is perceived, others are more active when their preferred image is suppressed, and yet others show little selectivity during nonrivalrous stimulation but become more selective during rivalrous stimulation (Leopold and Logothetis, 1996; Logothetis, 1998; Logothetis and Schall, 1989).

Several explanations of binocular rivalry have been proposed (Dayan, 1998; Gomez et al., 1995; Lehky, 1988; Lumer, 1998). One set of theories propose that the alternation is due to some form of reciprocal inhibition between the two monocular pathways (Blake, 1989; Lehky, 1988). Many of the existing theories involve neural network or rate models for which making direct quantitative comparisons with neurophysiological recordings are not possible.

Our focus is on the specific biophysical mechanisms responsible for binocular rivalry and multistable perception. We present a network of Hodgkin-Huxley-type neurons that reproduces the observed psychophysical and experimental behavior. Our network consists of both excitatory and inhibitory cells in a biophysically plausible cortical network. We then present a reduced population rate model derived from the spiking neuronal network. We propose that the known observed phenomena associated with binocular rivalry are direct consequences of the underlying physiology of coupled spiking neurons.

We propose that a given percept is represented as a localized focus of active neurons (Hansel and Sompolinsky, 1998; Laing and Chow, 2001). In the simple case of the two presented images being oriented gratings (Lee and Blake, 1999; Logothetis et al., 1996), we suggest that a population of neurons is tuned to a given orientation, and neurons in this population are locally connected to other neurons with similar preferred orientations. (We note that our spiking model could be adapted so that the two foci represent eye images.) When a grating of a given orientation is presented, the network receives orientation-specific inputs, and the local cortical connectivity shapes the activity of the population to fire maximally at the preferred orientation with a drop off in activity away from the maximum in a way that matches the tuning curve of the individual neurons. One possibility is that this network is situated at a higher-level visual area, where inputs arrive both from lower level visual areas and from higher-level cortical areas.

When two conflicting stimuli are presented, the network is unable to sustain activity centered around both inputs simultaneously and thus alternates between one focus of activity and the other. This switching is the neurophysiological correlate of binocular rivalry. The switching is induced by a slow process such as spike frequency adaptation or synaptic depression. The dominance duration depends on not only the time scale of the slow process but also strongly on the input strength to the network. This allows for large variations in the dominance times even when the time-constant of the slow process is fixed. Our simulations and analysis show that the behavior of the network matches the observed behavior in a number of ways: (1) it reproduces the distribution of dominance durations seen in humans and primates, (2) there is a lack of correlation between lengths of successive dominance durations, (3) variation of stimulus strength to one eye influences only the mean dominance duration of the contralateral eye, not the mean dominance duration of the ipsilateral eye, (4) increasing both stimuli strengths in parallel decreases the mean dominance durations, and (5) rotating the bars so they are no longer orthogonal increases mean dominance durations. The model's behavior when the stimulus strength to one eye is changed in synchronization with either the suppression or dominance of the percept presented to that eye also agree with experimentally observed behavior.

Our model combines local cortical circuits and higher-level control to explain binocular rivalry. Local cortical circuits are responsible for selecting which neurons are involved in the particular perception and inducing the switching between the alternate perceptions. High-level feedback can play a role in setting the eventual mean dominance times and can strongly influence which image is perceived.

2. Hodgkin-Huxley Type Model

Our model consists of a network of excitatory and inhibitory Hodgkin-Huxley-type conductance-based neurons in a biophysical cortical network architecture. The neurons are orientation selective and receive external inputs from both eyes and possibly feedback from higher levels. They have a "preferred orientation" and fire at a high rate when presented with a grating at that orientation. To model the experiment in which the

two eyes are presented with orthogonal gratings, we inject currents at two locations in the network centered around neurons whose preferred orientations differ by 90 degrees. The spatial structure of the current input is Gaussian (see Fig. 1 and Eq. (20)). Note that since there is no eye-specific information in the network, this model is also appropriate for the study of monocular viewing of orthogonal sinusoidal gratings (Andrews and Purves, 1997; Walker, 1976). In these experiments, periods of mixed perception are intermingled with periods of exclusive visibility of one or the other pattern.

We assume that excitatory cells are synaptically coupled to other excitatory cells with a strength that decays as a Gaussian function of the difference between their preferred orientations. There is also coupling with a Gaussian footprint from excitatory neurons to inhibitory neurons, between inhibitory neurons, and from inhibitory neurons to excitatory neurons, with the variable always being the difference in preferred orientations. The equations and parameter values are given in the Methods section.

We include two slow processes. The first is spike frequency adaptation due to a calcium-dependent potassium current (Huguenard and McCormick, 1992; McCormick and Huguenard, 1992). This is sufficient to cause oscillations in the network's activity, although they occur on a similar time-scale to the time constant of the decay of this current, ∼80 ms. We also include synaptic depression in the excitatory to excitatory connections that has a larger time-constant (Abbott et al., 1997). We find that synaptic depression alone is not sufficient to cause switching: we need a slow hyperpolarizing current as well. The switching phenomenon is quite robust with respect to the exact strengths and time-scales of these slow variables.

For simplicity, we explicitly model only those neurons whose activity increases when their preferred stimuli are perceived. Those neurons that respond preferentially when their preferred stimuli are suppressed may be part of a different circuit that is involved in suppression of a particular image or eye, and those whose selectivity changes when the stimulus is changed from rivalrous to nonrivalrous may be manifesting the effects of attention on perception (Leopold and Logothetis, 1996; Logothetis, 1998; Logothetis and Schall, 1989). Neurons in these last two classes are not explicitly modeled. Those neurons possibly involved in suppressing an image are similar to those that fire when their preferred stimulus is dominant (both groups fire when one image is suppressed) and our model could be augmented to include such neurons.

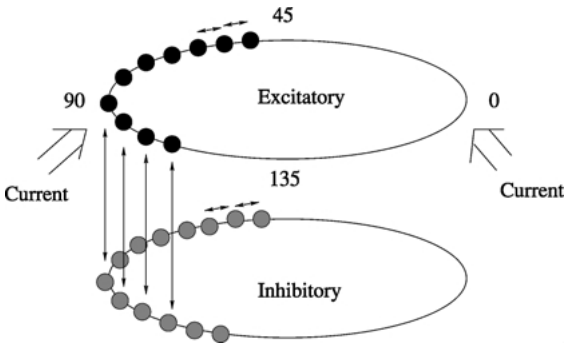

Figure 1. Two coupled networks of binocular, orientation-selective neurons. The neurons are labeled with their preferred orientation in degrees. Current is injected to two groups of neurons whose preferred orientations differ by 90 degrees.

2.1. Simulation Results

Figure 2 shows a rastergram of the firing events of the excitatory neurons in the network given two current

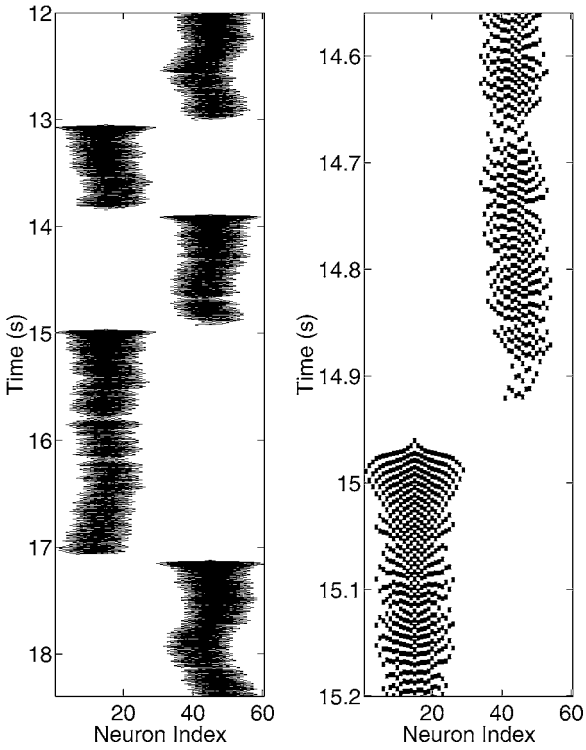

Figure 2. Activity in the excitatory population as a function of time. The current stimuli are centered at neurons 15 and 45. The right plot shows detail of the left plot.

stimuli centered at neurons whose preferred orientations differ by 90 degrees. At every moment in time, the activity is localized into a bump that is centered at either of the two locations of maximum external current input. A bump in one of these locations is thought to represent a perception of bars of the corresponding orientation. The inhibitory neuron activity is very similar although it has a greater angular spread. Note the wide spread of activity, lasting less than 100 ms, when the activity initially moves to another location. The decrease in width after this period is probably due to the adaptation current saturating. This type of high activity at the onset of a percept is seen in some neurons in superior temporal sulcus and inferior temporal cortex during binocular rivalry (Leopold and Logothetis, 1999; Sheinberg and Logothetis, 1997). Experimentally, bursting behavior is also seen in some of these neurons. Replacing some of the fast excitatory synapses in our model with slower NMDA-type synapses (as in Wang, 1999) causes neurons in a bump to burst in an approximately synchronous fashion while active, rather than fire approximately periodically and asynchronously (results not shown). The network is capable of sustaining only one bump at any given time, and since the neurons are coupled synaptically, the subthreshold inputs to the currently suppressed bump do not affect the currently active bump.

Figure 3 shows the voltage trace from a typical neuron in a bump. Note the slower firing rate at the end of a firing episode relative to that at the start. This simulation used a total of 60 excitatory and 60 inhibitory neurons and had no external noise. Similar switching behavior is seen when larger numbers of neurons are used, but we do not show results for these larger networks because of the prohibitively large amounts of computer time required for such simulations.

A histogram of dominance durations is shown in Fig. 4. It is unimodal and skewed, with a long tail at long durations. Included are fits to the data of a Gamma function that is commonly (Kovacs et al., 1996; Logothetis et al., 1996), although not always (Gomez et al., 1995; Lehky, 1995), fitted to such data, along with another function Eq. (12) that is derived in Section 3.1. Figure 5 shows the autocorrelation coefficients for the data in Fig. 4. The lack of any strong correlation beyond zero lag is clearly seen, in agreement with observations (Lehky, 1988, 1995; Logothetis et al., 1996). The Lathrop statistic (Logothetis et al., 1996), which measures the correlation between successive values in a time series, was calculated ($\bar{L} = 0.977$, $\sigma = 0.073$,

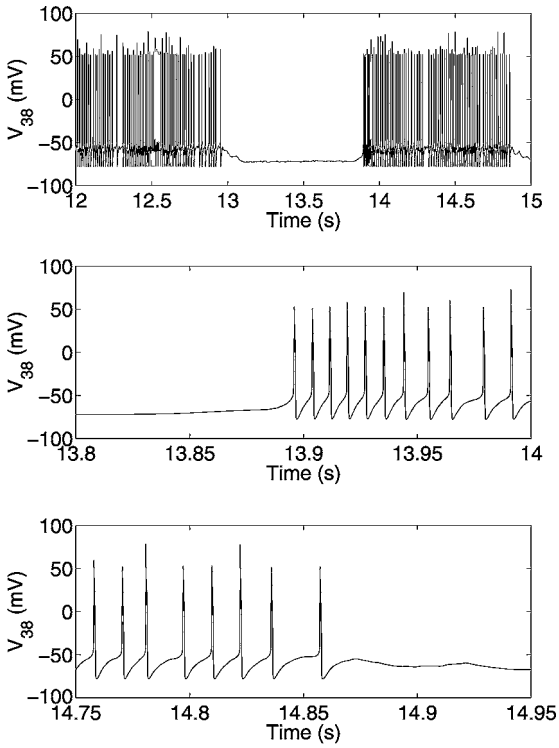

Figure 3. Voltage of the 38th neuron in Fig. 2. Note the different horizontal scales in the lower two plots. The apparent difference in spike heights is a result of plotting voltage at discrete values of time.

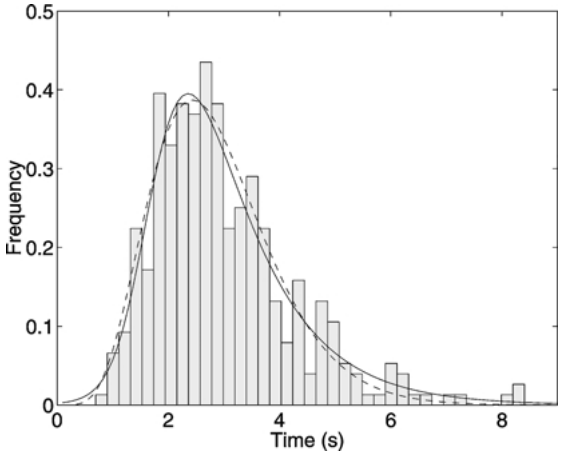

Figure 4. The distribution of dominance durations for the Hodgkin-Huxley model. The solid line is Eq. (12) with parameters $\gamma = 0.0174$, $\eta = -0.0005$, $\kappa = 0.0782$, $\tau = 1.1389$, and the dashed is a Gamma distribution with $\lambda = 2.3593$ and $r = 6.7381$, where the Gamma distribution is $f(t) = \lambda^r / \Gamma(r) t^{r-1} \exp(-\lambda t)$.

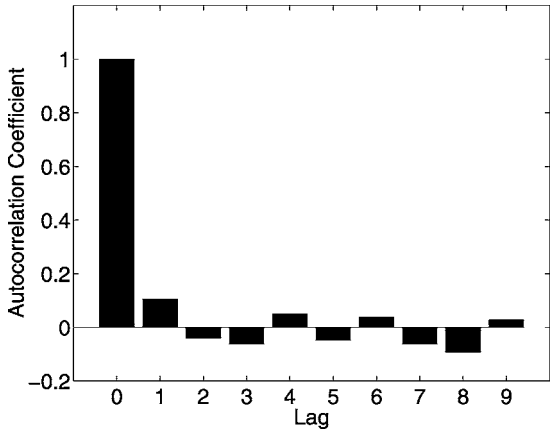

Figure 5. Autocorrelation coefficients for the data in Fig. 4.

giving a z value of 0.31), and this confirms the lack of a significant correlation. A simple explanation for this lack of correlation in a completely deterministic system is that the system is chaotic: the maximum Lyapunov exponent is approximately 40 s^{-1}. Since typical dominance durations are much longer than the reciprocal of this quantity, switching times can be thought of as resulting from an extreme "undersampling" of the underlying dynamical system, and successive dominance durations will not be correlated (Racicot and Longtin, 1997). This interpretation as undersampling also provides an explanation of the results of Lehky (1995) who, by analyzing a time series of dominance durations, concluded that the underlying dynamical system was not a low-dimensional chaotic attractor. Both Kalarickal and Marshall (2000) and Lehky (1988) studied simple models of binocular rivalry that showed this lack of serial correlation, but both models had stochastic inputs.

As a result of the spatial structure of both the external current inputs and the coupling, neurons in the network have a range of different input currents and hence fire at different average frequencies (Hansel and Sompolinsky, 1998; Laing and Chow, 2001). Thus, the neurons cannot synchronize, and there should not be any strong correlations between firing times of different neurons although weak correlations are possible (Gutkin et al., 2001). As the number of neurons in the network increases, fluctuations in the synaptic input to a given neuron should decrease. The observed nonzero variance of experimentally obtained distributions is thought to be due to both fluctuations from the finite number of neurons in the network and synaptic, channel or external noise.

The switching can be understood heuristically. In Section 3 we give a more quantitative explanation. Consider two input stimuli 1 and 2. Connections between excitatory neurons promote activity centered at stimulus 1 or 2, while inputs from the inhibitory population prevent this activity from spreading over the whole network. This inhibitory activity is also strong enough to suppress activity at the site corresponding to the stimulus that is not perceived. (For sufficiently strong inputs, two bumps may coexist). Suppose that population 1 is active and 2 is suppressed, and consider the effects of the slow current responsible for spike frequency adaptation. This current increases at site 1 and decreases at site 2 until eventually the adaptation remaining from activity at site 2 has decreased sufficiently that the neurons at site 2 are able to fire again, immediately suppressing the neurons at site 1. The adaptation current at site 2 then builds up, the adaptation current at site 1 wears off sufficiently, and the cycle repeats. A similar argument can be made if synaptic depression is the cause of the switching: both the recurrent excitation at site 1 and the inhibition of the neurons at site 2 weaken, allowing neurons at site 2 to fire and suppress neurons at site 1.

One well-known aspect of binocular rivalry is that if the strength of the stimulus to one eye is changed, it is largely the mean dominance duration of the other eye that is affected, not the mean dominance duration of the eye whose stimulus strength is being changed. This effect is sometimes known as Levelt's second proposition (Bossink et al., 1993; Levelt, 1968) and has been observed many times (Leopold and Logothetis, 1996; Logothetis et al., 1996; Mueller and Blake, 1989). More specifically, if the strength of the stimulus to eye 1 is decreased, the mean dominance duration of eye 2 typically increases markedly in a nonlinear fashion, while the mean dominance duration of eye 1 decreases by a small amount. We performed this experiment with our model, and the results are shown in Fig. 6 (together with data from the reduced model that is presented in Section 3). They agree well with observations, and an explanation for this behavior is given in Section 3.

Another experiment that has been performed involves changing the angle between the two sets of bars presented to the two eyes. It has been observed that decreasing the angle from 90 degrees causes the mean dominance durations to increase (Andrews and Purves, 1997). We performed this experiment on our model, and the results are shown in Fig. 7. The variation is small (as it is in experiments) (Andrews and Purves,

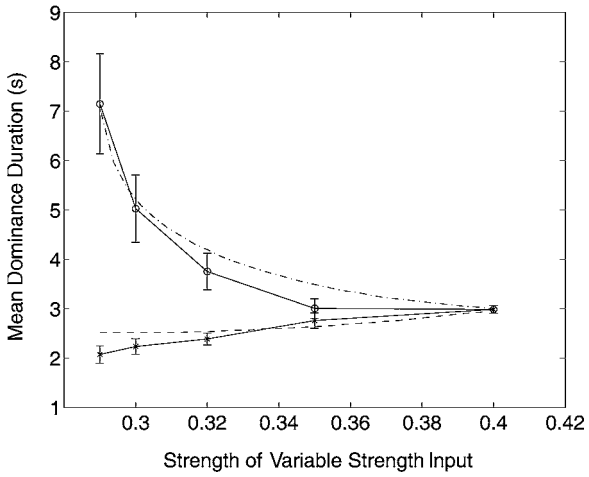

Figure 6. A demonstration of Levelt's second proposition in a spiking neuron model. The strength of one input was fixed at 0.4 and the other was reduced. × is mean dominance duration for the stimulus whose strength was decreased, ○ is mean dominance duration for the stimulus whose strength was unchanged. Compare with Leopold and Logothetis (1996, Fig. 1), Logothetis et al. (1996, Fig. 4), or Mueller and Blake (1989, Fig. 2). Also shown are rescaled dominance durations from the reduced model (1) through (6) (dashed and dash-dotted). See text for details.

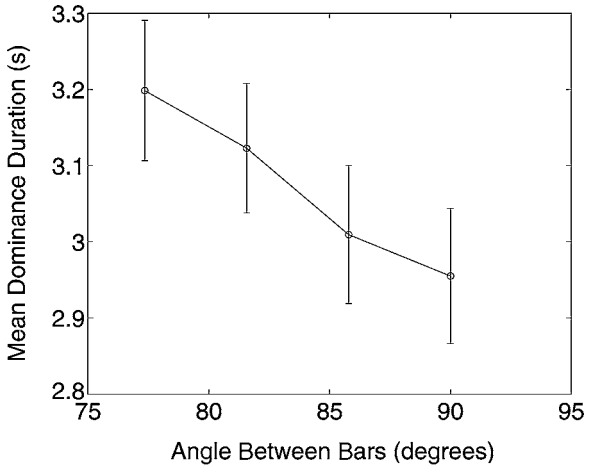

Figure 7. Variation of mean dominance duration as a function of the angle between two sets of gratings presented to the two eyes. Smaller angular differences could not be tested, since for these values the two bumps "merged." The bars indicate the standard deviation of the dominance durations. Compare with Andrews and Purves (1997, Fig. 4B(i)).

1997) but significant. Smaller angular differences could not be tested, as this caused the two bumps to "merge" into one that spanned both input positions. This is due to the widths of the Gaussians used in coupling neurons. If these widths were reduced, smaller angular differences could have been tested, but the total number of neurons in the network would have then had to be correspondingly increased, resulting in prohibitively long simulation times. An explanation for the dependence of dominance duration on angle between bars is given in Section 3.

A further experiment of interest is that of Mueller and Blake (1989). They changed the strength (contrast) of the stimulus presented to one eye, but the change was only made during either dominance or suppression of that image. For example, if the manipulation is synchronized with dominance of an eye, the contrast of the image presented to that eye is changed when that image is reported as being dominant and is returned to the baseline level when the image is no longer reported as being dominant. We performed this experiment with our model, and the results are shown in Fig. 8. The

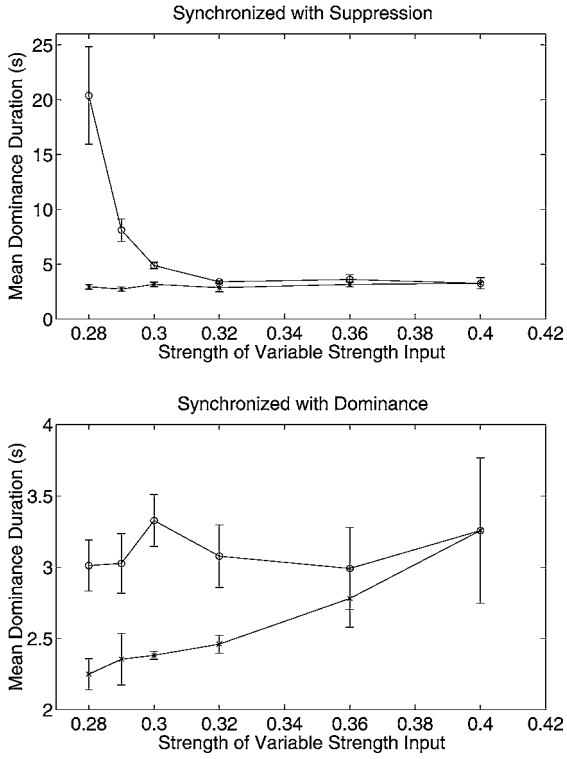

Figure 8. The effects of changing the strength of one input in the spiking neuron model, synchronized to either the suppression of that image (top) or the dominance of that image (bottom), as described by Mueller and Blake (1989). The strength of one input was fixed at 0.4, and the other was reduced. × is mean dominance duration for the stimulus whose strength was decreased, ○ is mean dominance duration for the stimulus whose strength was unchanged. Compare with Mueller and Blake (1989, Fig. 4).

results for the case where the stimulus strength is synchronized with suppression of that image (Fig. 8, top) are very similar to the situation described above as Levelt's second proposition—i.e., if the stimulus strength is decreased, the dominance duration of the ipsilateral eye is largely unaffected, but the dominance duration of the contralateral eye increases markedly (compare Fig. 8, top, with Fig. 6). The results shown in this figure agree well with experimental results (Mueller and Blake, 1989, Fig. 4). The case when the stimulus strength is synchronized with dominance of the image is shown in Fig. 8, bottom. It is seen that decreasing the stimulus strength slightly *decreases* the dominance duration of the ipsilateral eye but leaves the dominance duration of the contralateral eye essentially unchanged. This is also in good agreement with experimental results (Mueller and Blake, 1989). An explanation for this behavior is given in Section 3.

3. Reduced Description

We make our heuristic arguments more precise with a reduced spatially averaged model. The resulting equations are similar to the proposed models of Kalarickal and Marshall (2000), Lehky (1988), Mueller (1990), and Wilson et al. (2000). In Appendix B we describe how the following equations can be derived from our spiking neuronal network. They represent the spatially averaged dynamics of two populations of Hodgkin-Huxley-type neurons with recurrent excitation, cross-inhibition, adaptation, and synaptic depression:

$$\frac{du_1}{dt} = -u_1 + f(\alpha u_1 g_1 - \beta u_2 g_2 - a_1 + I_1) \tag{1}$$

$$\frac{du_2}{dt} = -u_2 + f(\alpha u_2 g_2 - \beta u_1 g_1 - a_2 + I_2) \tag{2}$$

$$\tau_a \frac{da_1}{dt} = -a_1 + \phi_a f(\alpha u_1 g_1 - \beta u_2 g_2 - a_1 + I_1) \tag{3}$$

$$\tau_a \frac{da_2}{dt} = -a_2 + \phi_a f(\alpha u_2 g_2 - \beta u_1 g_1 - a_2 + I_2) \tag{4}$$

$$\tau_d \frac{dg_1}{dt} = 1 - g_1 - g_1 \phi_d f(\alpha u_1 g_1 - \beta u_2 g_2 - a_1 + I_1) \tag{5}$$

$$\tau_d \frac{dg_2}{dt} = 1 - g_2 - g_2 \phi_d f(\alpha u_2 g_2 - \beta u_1 g_1 - a_2 + I_2), \tag{6}$$

where all constants are positive. Here u_i represents the spatially averaged net excitatory activity of each localized population seen in the simulations of the spiking neurons ($i = 1, 2$ labels the percept or "bump"), a_i and g_i are the population adaptation and synaptic depression variables, respectively. We have included synaptic depression in both the excitatory and inhibitory connections. While depression is thought to occur in only excitatory synapses, the inhibitory neurons in the full spiking model are largely driven by the excitatory population, and it is the depression in the excitatory to excitatory connections that leads to this decrease in inhibitory activity on the time-scale of the depression, so this is not an unreasonable choice. For simplicity we take the gain function f to be the Heaviside step function—i.e., $f(x) = 1$ for $x \geq 0$ and $f(x) = 0$ for $x < 0$. The constants τ_a and τ_d are the time constants of the adaptation and synaptic depression, respectively, and are both assumed to be much larger than 1. A high level of u_i is assumed to be directly correlated with the perception of image i. The chaotic dynamics of the spiking network are not represented in these reduced equations. They could be mimicked by including stochastic forcing terms.

The dynamics of (1) through (6) are fairly simple because of the separation of time-scales between the activities and the slow variables. Depending on the parameters, the system either oscillates or goes to a steady state. The only possible steady states are both activities at zero (both off), both activities at 1 (both on), or one at 1 and the other at zero (one on) and its mirror image.

For clarity, first consider the case where only adaptation is active (i.e., $g_1 = g_2 = 1$ and we ignore Eqs. (5) and (6)). For the both-off steady state, the variables satisfy $(u_1, u_2, a_1, a_2) = (0, 0, 0, 0)$. For this state to exist, the total inputs of the gain functions must be below threshold—i.e., $I_1 < 0$ and $I_2 < 0$. For the both-on fixed state, $(u_1, u_2, a_1, a_2) = (1, 1, \phi_a, \phi_a)$. In this case, the inputs must be greater than threshold—i.e., $\alpha - \beta - \phi_a + I_1 > 0$ and $\alpha - \beta - \phi_a + I_2 > 0$. Thus, strong inputs or strong excitation is required for the both-on state. The one-on case has $(u_1, u_2, a_1, a_2) = (1, 0, \phi_a, 0)$ or its mirror image. This requires $\alpha - \phi_a + I_1 > 0$ and $I_2 - \beta < 0$. Thus, the one-on fixed state needs strong excitation and inhibition compared to the inputs.

If none of the fixed-state conditions are satisfied, then the system oscillates. Say, for example, that $u_1 = 1$ and $u_2 = 0$. Then with a time constant τ_a, a_1 exponentially approaches ϕ_a and a_2 exponentially approaches zero. This will decrease the total inputs to u_1 and increase the total inputs to u_2. This causes the inputs to u_2 to cross threshold, making u_2 increase and simultaneously

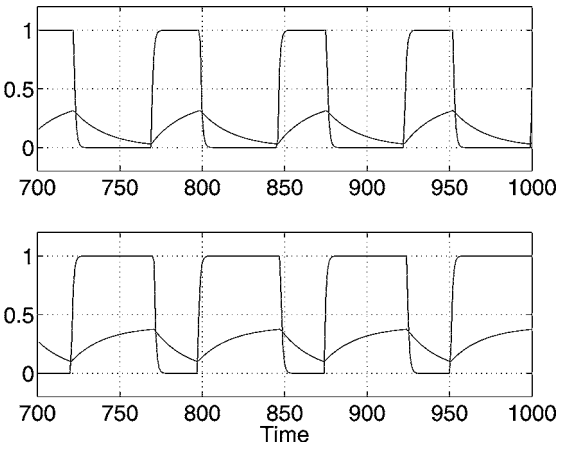

Figure 9. Solution of the reduced model (1) through (4). Parameter values are $\alpha = 0.2$, $\beta = 0.4$, $\phi_a = 0.4$, $\tau_a = 20$, $I_1 = 0.43$, $I_2 = 0.5$, $g_1 = g_2 = 1$. The top plot is u_1 and a_1, the bottom is u_2 and a_2.

increasing inhibition to u_1, causing it to decrease. The process then repeats and oscillations ensue. We equate the duration that each population is turned on with the dominance time of the corresponding percept.

An example is shown in Fig. 9. Parameter values are $\alpha = 0.2, \beta = 0.4, \phi_a = 0.4, \tau_a = 20, I_1 = 0.43, I_2 = 0.5$. One population becomes active only when its adaptation has worn off by a sufficient amount. For the parameters shown, population 1 switches on when $a_1 = I_1 - \beta = 0.03$ and population 2 switches on when $a_2 = I_2 - \beta = 0.1$.

We can calculate the dominance period by following the dynamics of the adaptation variable. It has a growing phase ($a_i(t) \equiv a_i^g(t)$) and a decaying phase ($a_i(t) \equiv a_i^d(t)$). Let T_1 be the dominance period of percept 1 (decay phase of a_2) and T_2 be that of percept 2 (decay phase of a_1). T_1 is obtained from the condition

$$I_2 - \beta - a_2^d(T_1) = 0, \tag{7}$$

where time is measured from the onset of percept 1. Solving (4) in the decaying phase gives $a_2^d(t) = a_2^d(0) \exp(-t/\tau_a)$. We need to compute $a_2^d(0)$. We first note that $a_2^g(t) = \phi_a + (I_2 - \beta - \phi_a)\exp(-t/\tau_a)$ in the growing phase, where time is now measured from the onset of percept 2, and that $a_2^d(0) = a_2^g(T_2)$. This yields

$$I_2 - \beta - [\phi_a + (I_2 - \beta - \phi_a)\exp(-T_2/\tau_a)] \times \exp(-T_1/\tau_a) = 0. \tag{8}$$

Repeating for a_1 we get the same equation but with the indices reversed. This then allows us to solve for T_1 and T_2 to obtain

$$\begin{aligned} T_1 &= -\tau_a \log\left(\frac{I_2 - \beta}{\beta + \phi_a - I_1}\right), \\ T_2 &= -\tau_a \log\left(\frac{I_1 - \beta}{\beta + \phi_a - I_2}\right). \end{aligned} \tag{9}$$

These are shown in Fig. 10, top. It is clear that T_1 is largely independent of I_1, while T_2 has a strong dependence on I_1. This is an explanation for Levelt's second proposition.

One notable difference between the curves in Fig. 10, top, and the data in Fig. 6 for the spiking neuron model (and also those reported in Leopold and Logothetis, 1996; Logothetis et al., 1996; and Mueller and Blake, 1989) is that T_1 increases as I_1 is decreased in (9), in contrast with the other results above. (The qualitative

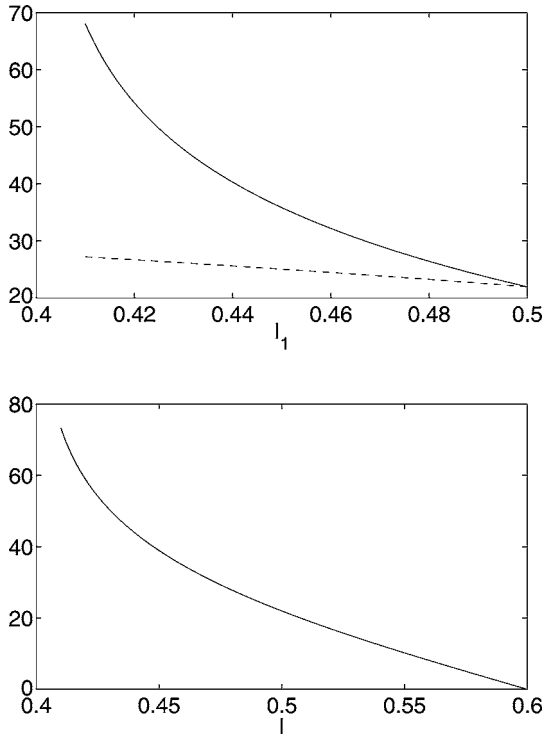

Figure 10. Dominance durations with only adaptation considered. Top: Eqs. (1) through (4) with $g_1 = g_2 = 1$, as given by (9). T_1 is dashed and T_2 is solid. Note the slight increase in T_1 as I_1 is decreased, in contrast with Fig. 6. Parameter values are $\alpha = 0.2$, $\beta = 0.4$, $\phi_a = 0.4$, $\tau_a = 20$, $I_2 = 0.5$. Bottom: Dominance duration as a function of input (I), when the inputs to (1) through (4) are equal (i.e., $I_1 = I_2 = I$). Other parameters are as above.

nature of the behavior predicted by (9) was also seen in the spiking neuron model when no synaptic depression was included; results not shown.) However, adding the effects of depression to those of adaptation in the model (1) through (6) can produce qualitative agreement between the behavior of T_1 as a function of I_1 for the reduced model, and the spiking model and experimental results mentioned above (see below).

From expressions (9) we can determine the dependence of dominance duration on input when the inputs have equal strength—i.e., $I_1 = I_2 = I$:

$$T = -\tau_a \log\left(\frac{I-\beta}{\beta+\phi_a-I}\right). \tag{10}$$

This is shown in Fig. 10, bottom. We see that as I is decreased, the dominance durations increase, as observed experimentally. Also, there is a critical value of I ($I=\beta$) such that for $I<\beta$ there are no oscillations.

The simple model (1) through (4) can also explain the results of Mueller and Blake (1989) regarding synchronized changes in input, and the results of their type of experiment on our detailed biophysical model (Fig. 8). Imagine that I_2 is fixed at I and that I_1 is also set to I when u_1 is high but is switched to $I-\Delta$ when u_1 is low—i.e., the change in I_1 is synchronized with the suppression of percept 1. Since T_1 is governed by the decay of a_2 to a value set by I_2 when u_2 is low, and T_2 is governed by the decay of a_1 to a value set by I_1 when u_1 is low, this manipulation will clearly affect T_2 more than it affects T_1. In fact, the expressions for T_1 and T_2 in this situation can be obtained directly from (9):

$$\begin{aligned} T_1 &= -\tau_a \log\left(\frac{I-\beta}{\beta+\phi_a-I+\Delta}\right), \\ T_2 &= -\tau_a \log\left(\frac{I-\Delta-\beta}{\beta+\phi_a-I}\right). \end{aligned} \tag{11}$$

Increasing Δ will produce a figure identical to Fig. 10, top, which is qualitatively the same as in Mueller and Blake (1989, Fig. 4A).

Conversely, if I_1 is changed to a new level when u_1 is high (i.e., the changes in I_1 are synchronized with the dominance of percept 1), it is clear from the arguments above that this will not affect either of the dominance durations. Experimentally (Mueller and Blake, 1989) and for simulations of our biophysical model (Fig. 8, bottom), dominance durations during this type of experiment show either weak or no significant dependence on the value to which I_1 is changed during the dominance of percept 1. Thus, while the reduced model (1) through (4) does not reproduce all experimental results in every detail, it does reproduce the overall behavior.

In the presence of synaptic depression alone, the dynamics are similar in the parameter regime with oscillations, although explicit expressions of the form (9) cannot be derived. As in the case of adaptation only, there is a relative lack of dependence of T_1 on I_1 (although it increases slightly as I_1 is decreased) and strong nonlinear dependence of T_1 on I_2 (not shown). However, in contrast with the adaptation-only model, once I decreases below the critical value for oscillations ($\beta/[1+\phi_d]$) the "both-on" state $((u_1, u_2, g_1, g_2) = (1, 1, 1/[1+\phi_d], 1/[1+\phi_d]))$ is stable (as is the "one-on" state, $(u_1, u_2, g_1, g_2) = (1, 0, 1/[1+\phi_d], 1)$ or its mirror image).

Using the reduced model above, we can explain why decreasing the angle between two sets of bars should increase the mean dominance durations. As mentioned, the inhibitory activity in the network of spiking neurons has a greater angular spread than the excitatory activity, so when the current inputs in Fig. 1 are moved closer to one another, the net effect is that each bump feels stronger inhibition from the other. For the rate model (1) through (6), this corresponds to increasing β, and from (10), or the equivalent expressions when only synaptic depression is considered, it can be see that this is equivalent to decreasing I, which leads to an increase in mean dominance duration.

For both spike frequency adaptation only and synaptic depression only we obtain a nonlinear dependence of the periods on stimulus strength, and the existence of a minimum strength for the weaker stimulus below which switching is not observed. The form of the dependencies are similar to those observed (Bossink et al., 1993; Leopold and Logothetis, 1996), however, when interpreting these results one should keep in mind that the relationship between "stimulus strength" and "current input" is not at all clear.

The full system, (1) through (6), shows qualitatively similar oscillations and dependence of dominance durations on input strengths as the two special cases examined above, and we suggest that in practice it may well be a combination of adaptation and synaptic depression (and possibly more than one mechanism for each of these) that causes switching. As a specific example of the behavior when both adaptation and depression are present in (1) through (6), we show in Fig. 6 linearly rescaled plots of T_1 (dashed) and T_2 (dash-dotted) as

functions of I_1 when I_2 was held constant. (Note that T_1 decreases as I_1 is decreased.) The parameter values are $\alpha = 0.35$, $\beta = 0.2$, $\phi_a = \phi_d = 0.6$, $\tau_a = 20$, $\tau_d = 40$, and the rescalings are $x = (0.11I_1 + 0.064)/0.27$ and $t = T_{1,2}/20 + 2.1$, where x is the strength of the current input for the spiking neuron model (Eq. (20)), and t is the dominance duration in seconds. Note that these rescalings can be absorbed into the parameters of the model (1) through (6), and do not represent any physical changes. The curves in Fig. 6 are not meant to be a fit to the data from the spiking model but to indicate that an appropriate mixture of adaptation and depression in the simple model (1) through (6) can qualitatively reproduce observed behavior.

This analysis shows that the dominance durations can vary over a wide range depending on the strength of the inputs. Thus even though the mechanism for switching may be adaptation, synaptic depression or a combination of these two, and these processes are likely to have relatively uniform time constants between subjects, there could still be wide variations in the dominance durations between subjects due to differences in actual input strengths. The sources of the binocular inputs in our model are not specified, and we envision them as being due to combined inputs from lower visual regions and higher cortical regions. We postulate that variations in these inputs could be the reason for the wide variation in dominance times seen in psychophysical experiments (Pettigrew and Miller, 1998).

3.1. Distribution of Dominance Durations

We can also use this reduced model to explain the distribution of dominance durations observed in the simulations of our spiking neuronal network. As noted in the above analysis, the switching of one percept to the other is controlled by the release from inhibition due to the decay back to the resting value of the adaptation or synaptic depression variable. If we include the effects of the fluctuations due to the chaotic dynamics (or noise effects), then this decay will be a stochastic process. Consider the example of adaptation only. During decay the adaptation current obeys $a^d(t) = a_0 \exp(-t/\tau)$. When a^d decays below a threshold level, the inhibited neurons will fire. However, with fluctuations the threshold value will be a stochastic variable, and a_0 will not be the same for each dominance period. Consider the simplified case where the threshold is reset to a random variable chosen from a Gaussian distribution, and a_0 is randomly chosen from another Gaussian distribution, each time a^d is reset. The distribution of dominance durations is then

$$p(T) = \Omega\left(\frac{e^{-T/\tau}[\gamma + \eta\kappa e^{-T/\tau}]}{[\gamma + \kappa e^{-2T/\tau}]^{3/2}}\right) \times \exp\left(\frac{-[e^{-T/\tau} - \eta]^2}{2(\gamma + \kappa e^{-2T/\tau})}\right), \qquad (12)$$

where Ω, γ, κ and η are related to the parameters of the two Gaussian distributions. See Appendix C for the derivation. This function is plotted in Fig. 4 together with data from the simulation of the full Hodgkin-Huxley network. It fits the data well and has the typical skewed shape seen in experimental data (Kovacs et al., 1996; Logothetis et al., 1996).

4. Discussion

Our cortical circuit of excitatory and inhibitory neurons is able to reproduce many of the observed dynamical characteristics of binocular rivalry. We are also able to compute analytically the dependence of the dominance period on the input strengths, and this shows how Levelt's second proposition can arise naturally in a network with mutual inhibition.

We find that the input strength to the network strongly influences the dominance duration. This allows large variations in the dominance durations even with fixed adaptation and synaptic depression timescales. The large distribution in mean times between subjects could be due to the differential input to the local circuit—this may be especially true of feedback from higher-level cortical areas—and the strength of this contribution could vary widely between subjects and even change within a subject. The neuromodulators acetylcholine, histamine, norepinepherin, and serotonin are all known to decrease the effects of spike frequency adaptation in human cortex (McCormick and Williamson, 1989), and if adaptation is the main mechanism for switching, changes in their concentration would significantly affect mean dominance durations. It is known that there is some training effect in binocular rivalry and multistable perception (Leopold and Logothetis, 1999), and systematic changes in switching frequency on the time-scale of several minutes have been observed (Borsellino et al., 1972; Lehky, 1995). Also, knowledge that a stimulus is ambiguous and has more than one possible perception plays a role in switching (Rock et al., 1994).

There are instances when rivalry does not take place. It is known that if the stimulus contrast is reduced, the images from the two eyes can fuse into a single merged percept (Leopold and Logothetis, 1999). Presumably, this fixed percept corresponds to a "fixed" pattern of activation. In our model, reducing the input stimulus causes the duration periods to increase until rivalrous oscillations cease. The ensuing fixed state depends on the type of slow process in the system. If only adaptation is included, then the network goes to the both-off state. If only depression is included, then the network can go into either the both-on state or the one-on state. With a combination of adaptation and depression either of the fixed states are possible. However, since our network is assumed to represent binocular information about orientation of gratings, it is unclear how fusion would be represented: it may not simply be a state where the network is in the "both-on" state. The local network we model may only represent the orientation of images, and the perception of grid images may be represented by a different set of neurons. One possible scenario is that the orientation network, when active, inhibits the network of grid neurons. Fusion then arises when the orientation network is inactive, thereby releasing the inhibition on the grid network. In this scenario, the both-off state in our network would correspond to fusion.

A lack of rivalry also occurs if the angular sizes of the images are increased beyond a given level. What is perceived instead is a constantly changing spatial patchwork of both images (Blake, 1989) or a traveling wave if the image is restricted to an essentially one-dimensional annulus (Wilson et al., 2001). Our cortical network may represent orientation for only a single spatial location, and the spatial patchwork may arise if there are many networks of the type we have studied, each corresponding to a different spatial location, and there is some form of local coupling between such networks. For strong input strength, either both-on or one-on states are possible in our model.

Our simulations show that switching caused by depression is much less robust to noise than switching caused by adaptation. The reason for this is probably that if depression is used, the switching occurs because the balance between excitation and inhibition gradually changes during a dominance period, finally reaching a critical value. This balance is quite fragile, and external noise will upset it, causing switching. However, switching caused by the wearing off of adaptation in the form of a slow hyperpolarizing current seems more robust since the network will not switch until the current is close to threshold. Small to moderate amounts of noise will not change the magnitude of the current that is wearing off, acting instead to make the threshold a stochastic function of time rather than a constant. One modification of the depression mechanism that could make it more robust is the inclusion of not only depression between excitatory neurons, but facilitation in the connections from excitatory to inhibitory neurons (Markram et al., 1998), on an appropriate time-scale. We have seen that both adaptation and depression have advantages and disadvantages with regards to modeling binocular rivalry, and in practice it is likely that they both contribute. It is worth noting that in both the spiking neuron and reduced models, the only way to obtain the correct dependence of the mean dominance duration of the ipsilateral eye on stimulus strength when testing Levelt's second proposition was to include both spike frequency adaptation and synaptic depression. This suggests that both are present in the relevant circuits of the cortex.

Our reduced model was anticipated by Lehky (1988), who proposed a neural network model of binocular rivalry that involved reciprocal inhibitory feedback between signals from the two eyes, prior to binocular convergence. He created an electronic circuit to represent the network, and for strong enough reciprocal inhibition the circuit oscillated. The oscillations stopped for weak inhibition, which Lehky attributed to fusion. He could reproduce Levelt's second proposition by changing the adaptation rates on either neuron and postulated that changing stimulus strength changes adaptation rates.

Recently, Kalarickal and Marshall (2000) numerically studied a model similar to (1) through (6), with noise but not including adaptation. Their model reproduced Levelt's second proposition, the lack of correlation between successive dominance durations, and the results of Mueller and Blake (1989) relating to synchronized changes in input strengths. They also realized that it is the total input to the inactive population that determines the time for which the active population remains active (thus explaining Levelt's second proposition and the results of Mueller and Blake, 1989), but the advantage of our reduced model (1) through (6) over their model is that the dependence of dominance duration on input can be explicitly derived.

Mueller (1990) presented a reduced model similar to (1) through (6) but without noise and by trial and error chose parameters so that his model reproduced the

results of Mueller and Blake (1989). However, due to the complexity of his model, little analytical insight can be gained regarding the mechanisms or the underlying physiology.

Wilson et al. (2000) studied the oscillations in the perception of circles in static periodic dot patterns (Marroquin patterns) using a planar network of 64 by 64 coupled "spike-rate" units, each of which is analogous to our rate model (1) through (6), although these authors did not include synaptic depression. Their adaptation variable's time-constant determines the slow (on the order of a few seconds) perceived switching between circles. They also fit a Gamma function to their distribution of dominance periods. They did not include noise in the simulations, so the width of the histogram of observed dominance periods is due to the complex, possibly chaotic, behavior of a high-dimensional dynamical system.

A third alternative model that we could have studied is a spatially extended rate model, similar to that of Wilson et al. (2000). Using Gaussian connectivity similar to that used in the Hodgkin-Huxley-type model (see Appendix A), but using rate units with dynamics similar to (1) through (6), we obtain bumps similar to those seen in other rate models (Hansel and Sompolinsky, 1998; Laing and Chow, 2001). By adding spatially inhomogeneous currents and enough adaptation and/or depression, we obtain bumps that alternate in a way similar to those shown in Fig. 2 (results not shown). The main difference between a spatially extended rate model and a spatially extended spiking neuron model is that alternation of bumps in the former is strictly periodic (as it is in, e.g., Dayan, 1998), whereas in the latter it is nonperiodic, as seen from Fig. 4. Thus such a model provides few benefits over a spatially averaged rate model such as (1) through (6).

Our model does not specify whether the rivalry is "stimulus rivalry" or "eye rivalry." Recent results of Lee and Blake (1999) may indicate that both are occurring. These authors presented orthogonal gratings to the two eyes and investigated the effects of both flickering the images at 18 Hz and swapping the images between the two eyes (as done by Logothetis et al., 1996). Their results suggest that both the 18 Hz flicker and the swapping of the images continually produce transient effects that significantly change perception of the images, and that either "eye rivalry" or "stimulus rivalry" can result from very similar stimuli. Other recent results (O'Shea, 1998) suggest that binocular rivalry consists of two components: alternations between two images that are independent of eye of origin and alternations between two images that depend on eye of origin. It is possible that networks with our proposed connectivity exist in various regions of the cortex and produce rivalrous dynamics.

The temporal dynamics of the perception of other ambiguous stimuli such as the Necker cube are similar to those investigated in this model (Borsellino et al., 1972; Gomez et al., 1995), which lends weight to the idea that binocular rivalry is another manifestation of competition between alternative representations of a stimulus, rather than being a phenomenon that is restricted to the ocular system (Leopold and Logothetis, 1999), and it may be possible to extend this type of modeling to include more complex visual stimuli, for example, blurred images (O'Shea et al., 1997).

Appendix A: Methods

The equations are (for each of the excitatory neurons)

$$\begin{aligned}
C\frac{dV_e}{dt} &= I_{syn} + I_{ext}(t) - I_{mem}(V_e, n_e, h_e) \\
&\quad - I_{AHP}(V_e, [Ca]) \\
\frac{dn_e}{dt} &= \psi[\alpha_n(V_e)(1-n_e) - \beta_n(V_e)n_e] \\
\frac{dh_e}{dt} &= \psi[\alpha_h(V_e)(1-h_e) - \beta_h(V_e)h_e] \\
\tau_e\frac{ds_e}{dt} &= A\sigma(V_e)(1-s_e) - s_e \qquad (13) \\
\frac{d[Ca]}{dt} &= -0.002 g_{Ca}(V_e - V_{Ca})/ \\
&\quad (1+\exp\{-(V_e+25)/2.5\}) - [Ca]/80 \\
\tau_g\frac{d\phi}{dt} &= 1 - \phi - f\sigma(V_e)\phi,
\end{aligned}$$

where $I_{mem}(V_e, n_e, h_e) = g_L(V_e - V_L) + g_K n_e^4(V_e - V_k) + g_{Na}(m_\infty(V_e))^3 h_e(V_e - V_{Na})$ and $I_{AHP}(V_e, [Ca]) = g_{AHP}[Ca]/([Ca]+1)(V_e - V_K)$. Other functions are $m_\infty(V) = \alpha_m(V)/(\alpha_m(V) + \beta_m(V))$, $\alpha_m(V) = 0.1(V+30)/(1-\exp\{-0.1(V+30)\})$, $\beta_m(V) = 4\exp\{-(V+55)/18\}$, $\alpha_n(V) = 0.01(V+34)/(1-\exp\{-0.1(V+34)\})$, $\beta_n(V) = 0.125\exp\{-(V+44)/80\}$, $\alpha_h(V) = 0.07\exp\{-(V+44)/20\}$, $\beta_h(V) = 1/(1+\exp\{-0.1(V+14)\})$, $\sigma(V) = 1/(1+\exp\{-(V+20)/4\})$.

Parameters are $g_L = 0.05$, $V_L = -65$, $g_K = 40$, $V_K = -80$, $g_{Na} = 100$, $V_{Na} = 55$, $V_{Ca} = 120$, $g_{AHP} = 0.05$, $\psi = 3$, $\tau_e = 8$, $\tau_g = 1000$. f had various values

between 0.5 and 1.5. The equations for the inhibitory neurons are

$$\begin{aligned} C\frac{dV_i}{dt} &= I_{syn} + I_{ext}(t) - I_{mem}(V_i, n_i, h_i) \\ \frac{dn_i}{dt} &= \psi[\alpha_n(V_i)(1-n_i) - \beta_n(V_i)n_i] \\ \frac{dh_i}{dt} &= \psi[\alpha_h(V_i)(1-h_i) - \beta_h(V_i)h_i] \\ \tau_i\frac{ds_i}{dt} &= A\sigma(V_i)(1-s_i) - s_i. \end{aligned}$$

$\tau_i = 10$ and other functions are as above. The synaptic current to the jth excitatory neuron is

$$\frac{1}{N}\left[\left(V_{ee} - V_e^j\right)\sum_{k=1}^{N} g_{ee}^{jk} s_e^k \phi^k + \left(V_{ie} - V_e^j\right)\sum_{k=1}^{N} g_{ie}^{jk} s_i^k\right], \tag{14}$$

where $V_{ee} = 0$, $V_{ie} = -80$, V_e^j is the voltage of the jth excitatory neuron, $s_{e/i}^k$ is the strength of the synapses emanating from the kth excitatory/inhibitory neuron, ϕ^k is the factor by which the kth excitatory neuron is depressed, N is the number of excitatory neurons (and the number of inhibitory neurons),

$$g_{ee}^{jk} = \alpha_{ee}\sqrt{\frac{50}{\pi}}\exp(-50[(j-k)/N]^2), \tag{15}$$

and

$$g_{ie}^{jk} = \alpha_{ie}\sqrt{\frac{20}{\pi}}\exp(-20[(j-k)/N]^2). \tag{16}$$

Similarly, the synaptic current entering the jth inhibitory neuron is

$$\frac{1}{N}\left[\left(V_{ei} - V_i^j\right)\sum_{k=1}^{N} g_{ei}^{jk} s_e^k + \left(V_{ii} - V_i^j\right)\sum_{k=1}^{N} g_{ii}^{jk} s_i^k\right], \tag{17}$$

where $V_{ei} = 0$, $V_{ii} = -80$, V_i^j is the voltage of the jth inhibitory neuron,

$$g_{ei}^{jk} = \alpha_{ei}\sqrt{\frac{20}{\pi}}\exp(-20[(j-k)/N]^2) \tag{18}$$

and

$$g_{ii}^{jk} = \alpha_{ii}\sqrt{\frac{30}{\pi}}\exp(-30[(j-k)/N]^2). \tag{19}$$

A typical I_{ext} for the excitatory population is

$$I(i) = 0.4\left[\exp\left(-\left\{\frac{20(i - N/4)}{N}\right\}^2\right) + \exp\left(-\left\{\frac{20(i - 3N/4)}{N}\right\}^2\right)\right] - 0.01, \tag{20}$$

where $i = 1 \ldots N$—i.e., two Gaussians centered at 1/4 and 3/4 of the way around the domain together with a constant negative current. I_{ext} for the inhibitory population is 0. Typical values for the coupling strengths are $\alpha_{ee} = 0.285$, $\alpha_{ie} = 0.36$, $\alpha_{ei} = 0.2$, $\alpha_{ii} = 0.07$.

Appendix B: Derivation of Reduced Model

Here we derive the reduced model, Eqs. (1) through (6). We first note that spike frequency adaptation and synaptic depression are both slow processes relative to the time over which a spike occurs. Both are driven by the postsynaptic activity. Focusing on adaptation we can write

$$\frac{da_i}{dt} = -a_i/\tau + A_i(t), \tag{21}$$

where a_i is a generalized adaptation variable (e.g., the calcium concentration in system (13)) and $A_i(t)$ is proportional to the cell activity (instantaneous firing rate) of neuron i. We then assume that the neuronal activity is driven by the synaptic inputs through a gain function f,

$$A_i(t) = f\left(\sum w_{ij}U_j(t) - a_i + I_i\right), \tag{22}$$

where w_{ij} represents the synaptic weight from neuron j to neuron i, and $U_j(t)$ is the postsynaptic response of neuron j. We assume that the influence of the adaptation is linear and I_i represents the external inputs to the neuron. A similar set of equations can be derived for a generalized synaptic depression variable.

If the postsynaptic response is stereotypical, we can write it as being induced by the activity through a linear filter yielding (Ermentrout, 1998)

$$U_j(t) = \int_{-\infty}^{t} \epsilon(t-s)A_j(s)\,ds. \tag{23}$$

If $\epsilon(t)$ is composed of exponential and power functions, we can invert this integral operator to obtain a differential equation for $U_j(t)$. For example, if we assume that $\epsilon(t)$ is given by a single exponential, then (23)

can be converted into a first-order differential equation. Substituting A_i from (22) into (23) we obtain a set of coupled differential equations involving the U_i's only, and we have converted the conductance-based network into a network of "rate" neurons.

We assume that the network is in a state of binocular rivalry where two bumps of neurons alternate their firing. The connectivity pattern of the network is such that the local inhibition has a broader footprint than the excitation. Within a given bump the excitation dominates the inhibition, but outside of the bump the opposite is true. We can thus consider the dynamics of a spatially averaged net activity of a bump that is self-exciting and inhibits another self-exciting bump. Labeling the two populations by 1 and 2 and including noise, we obtain the set of spatially averaged Eqs. (1) through (6).

Appendix C: Derivation of Dominance Duration Distribution

Assume that the slow variable decays as $g(t) = ae^{-t/\tau}$ toward a fixed threshold, θ, that has been chosen from a Gaussian with mean μ_θ and standard deviation σ_θ. The probability density function for θ is

$$f(\theta) = \frac{1}{\sigma_\theta\sqrt{2\pi}} \exp\left(\frac{-(\mu_\theta - \theta)^2}{2\sigma_\theta^2}\right), \tag{24}$$

so the conditional probability, $p(T \mid a)$, that the decay takes time T given the initial value a is proportional to

$$f(g(T))\left|\frac{dg}{dt}\right|_{t=T} = \left(\frac{ae^{-T/\tau}}{\tau\sigma_\theta\sqrt{2\pi}}\right)\exp\left(\frac{-(\mu_\theta - ae^{-T/\tau})^2}{2\sigma_\theta^2}\right). \tag{25}$$

If we now assume that the initial value, a, also comes from a Gaussian distribution with mean μ_a and standard deviation σ_a, the probability density function for T is

$$p(T) = \Omega\int_{-\infty}^{\infty} ae^{-T/\tau}\exp\left(\frac{-(\mu_\theta - ae^{-T/\tau})^2}{2\sigma_\theta^2}\right) \times \exp\left(\frac{-(\mu_a - a)^2}{2\sigma_a^2}\right)da \tag{26}$$

$$= \Omega e^{-T/\tau}\int_{-\infty}^{\infty} a \times \exp\left(-\left[A\left(a - \frac{B}{2A}\right)^2 + C - \frac{B^2}{4A}\right]\right)da, \tag{27}$$

where

$$A = \frac{e^{-2T/\tau}}{2\sigma_\theta^2} + \frac{1}{2\sigma_a^2}, \quad B = \frac{\mu_a}{\sigma_a^2} + \frac{\mu_\theta e^{-T/\tau}}{\sigma_\theta^2}, \quad C = \frac{\mu_\theta^2}{2\sigma_\theta^2} + \frac{\mu_a^2}{2\sigma_a^2} \tag{28}$$

and Ω is a normalization constant defined through $\int_{-\infty}^{\infty} p(T)\,dT = 1$. So

$$p(T) = \Omega e^{-T/\tau}e^{B^2/(4A)-C}\int_{-\infty}^{\infty} a \times \exp\left(-A\left(a - \frac{B}{2A}\right)^2\right)da \tag{29}$$

$$= \Omega e^{-T/\tau}e^{B^2/(4A)-C}\int_{-\infty}^{\infty}\left(u + \frac{B}{2A}\right)e^{-Au^2}\,du \tag{30}$$

$$= \frac{\sqrt{\pi}B\Omega e^{-T/\tau}e^{B^2/(4A)-C}}{2A^{3/2}}, \tag{31}$$

where we have made the substitution $u = a - B/(2A)$ and used the fact that ue^{-Au^2} is an odd function. Simplifying, we obtain

$$p(T) = \frac{\Omega\sigma_a\sigma_\theta\sqrt{2\pi}e^{-T/\tau}\left[\mu_a\sigma_\theta^2 + \mu_\theta\sigma_a^2e^{-T/\tau}\right]}{\left[\sigma_\theta^2 + \sigma_a^2e^{-2T/\tau}\right]^{3/2}} \times \exp\left(\frac{-[\mu_a e^{-T/\tau} - \mu_\theta]^2}{2\left(\sigma_\theta^2 + \sigma_a^2e^{-2T/\tau}\right)}\right). \tag{32}$$

Defining $\hat{\Omega} \equiv \Omega\sigma_a\sigma_\theta\sqrt{2\pi}$, $\gamma \equiv \sigma_\theta^2/\mu_a^2$, $\eta \equiv \mu_\theta/\mu_a$ and $\kappa \equiv \sigma_a^2/\mu_a^2$, this becomes

$$p(T) = \hat{\Omega}\left(\frac{e^{-T/\tau}[\gamma + \eta\kappa e^{-T/\tau}]}{[\gamma + \kappa e^{-2T/\tau}]^{3/2}}\right) \times \exp\left(\frac{-[e^{-T/\tau} - \eta]^2}{2(\gamma + \kappa e^{-2T/\tau})}\right). \tag{33}$$

Dropping the hat on Ω, this is Eq. (12).

Acknowledgments

This work was supported in part by grants from the National Institutes of Health and the Alfred P. Sloan Foundation to CCC. We are grateful to Hugh Wilson and Wulfram Gerstner for comments on the manuscript.

References

Abbott LF, Varela JA, Sen K, Nelson SB (1997) Synaptic depression and cortical gain control. Science 275: 220–223.

Andrews TJ, Purves D (1997) Similarities in normal and binocularly rivalrous viewing. Proc. Natl. Acad. Sci. USA 94: 9905–9908.

Blake R (1989) A neural theory of binocular vision. Psychol. Rev. 96: 145–167.

Borsellino A, De Marco A, Allazetta A, Rinesi S, Bartolini B (1972) Reversal time distributions in the perception of visual ambiguous stimuli. Kybernetik 10: 139–144.

Bossink CJH, Stalmeier PFM, De Weert CMM (1993) A test of Levelt's second proposition for binocular rivalry. Vision Res. 33: 1413–1419.

Carlson TA, He S (2000) Visible binocular beats from invisible monocular stimuli during binocular rivalry. Curr. Biol. 10(17): 1055–1058.

Dayan P (1998) A hierarchical model of binocular rivalry. Neural Comput. 10: 1119–1135.

Ermentrout GB (1998) Neural networks as spatio-temporal pattern-forming systems. Rep. Prog. Phys. 61: 353–430.

Fox R, Herrmann J (1967) Stochastic properties of binocular rivalry alternations. Percept Psychophys. 2: 432–436.

Gomez C, Argandona ED, Solier RG, Angulo JC, Vazquez M (1995) Timing and competition in networks representing ambiguous figures. Brain Cogn. 29: 103–114.

Gutkin BS, Laing CR, Colby CL, Chow CC, Ermentrout GB (2001) Turning on and off with excitation: The role of spike timing in asynchrony and synchrony in sustained neural activity. J. Comput. Neurosci. 11(2).

Hansel D, Sompolinsky H (1998) Modeling feature selectivity in local cortical circuits. In: C Koch, I Segev, eds. Methods in Neuronal Modeling (2nd ed.). MIT Press, Cambridge, MA.

Huguenard JR, McCormick DA (1992) Simulation of the currents involved in rhythmic oscillations in thalamic relay neurons. J. Neurophysiol. 68(4): 1373–1383.

Kalarickal GJ, Marshall JA (2000) Neural model of temporal and stochastic properties of binocular rivalry. Neurocomput. 32: 843–853.

Kovacs I, Papathomas TV, Yang M, Feher A (1996) When the brain changes its mind: Interocular grouping during binocular rivalry. Proc. Natl. Acad. Sci. USA 93: 15508–15511.

Laing CR, Chow CC (2001) Stationary bumps in networks of spiking neurons. Neural Comput. 13: 1473–1494.

Lee S-H, Blake R (1999) Rival ideas about binocular rivalry. Vision Res. 39: 1447–1454.

Lehky SR (1988) An astable multivibrator model of binocular rivalry. Perception 17: 215–228.

Lehky SR (1995) Binocular rivalry is not chaotic. Proc. R. Soc. Lond. B Biol. Sci. 259: 71–76.

Leopold DA, Logothetis NK (1996) Activity changes in early visual cortex reflect monkeys' percepts during binocular rivalry. Nature 379: 549–553.

Leopold DA, Logothetis NK (1999) Multistable phenomena: Changing views in perception. Trends Cogn. Sci. 3(7): 254–264.

Levelt WJM (1968) On Binocular Rivalry. Minor Series 2. Psychological Studies. The Hague: Mouton.

Logothetis NK (1998) Single units and conscious vision. Philos. Trans. R. Soc. Lond. B Biol. Sci. 353: 1801–1818.

Logothetis NK, Leopold DA, Sheinberg DL (1996) What is rivalling during binocular rivalry? Nature 380: 621–624.

Logothetis NK, Schall JD (1989) Neuronal correlates of subjective visual perception. Science 245: 761–763.

Lumer ED (1998) A neural model of binocular integration and rivalry based on the coordination of action-potential timing in primary visual cortex. Cereb. Cortex 8: 553–561.

Lumer ED, Friston KJ, Rees G (1998) Neural correlates of perceptual rivalry in the human brain. Science 280: 1930–1934.

Markram H, Wang Y, Tsodyks M (1998) Differential signaling via the same axon of neocortical pyramidal neurons. Proc. Natl. Acad. Sci. USA 95: 5323–5328.

McCormick DA, Huguenard JR (1992) A model of the electrophysiological properties of thalamocortical relay neurons. J. Neurophysiol. 68(4): 1384–1400.

McCormick DA, Williamson A (1989) Convergence and divergence of neurotransmitter action in human cerebral cortex. Proc. Natl. Acad. Sci. USA 86: 8098–8102.

Mueller TJ (1990) A physiological model of binocular rivalry. Vis. Neurosci. 4: 63–73.

Mueller TJ, Blake R (1989) A fresh look at the temporal dynamics of binocular rivalry. Biol. Cyber. 61: 223–232.

Ngo TT, Miller SM, Liu GB, Pettigrew JD (2000) Binocular rivalry and perceptual coherence. Curr. Biol. 10(4): R134–R136.

O'Shea RP (1998) Effects of orientation and spatial frequency on monocular and binocular rivalry. In: N Kasabov, R Kozma, K Ko, R O'Shea, G Coghill, T Gedeon, eds. Proceedings of the Fourth International Conference on Neural Information Processing and Intelligent Information Systems. Springer-Verlag, Singapore. pp. 67–70.

O'Shea RP, Govan DG, Sekuler R (1997) Blur and contrast as pictorial depth cues. Perception 26: 599–612.

Pettigrew JD, Miller SM (1998) A "sticky" interhemispheric switch in bipolar disorder? Proc. R. Soc. Lond. B Biol. Sci. 265: 2141–2148.

Racicot DM, Longtin A (1997) Interspike interval attractors from chaotically driven neuron models. Physica D 104: 184–204.

Rock I, Hall S, Davis J (1994) Why do ambiguous figures reverse? Acta Psychol. 87: 33–57.

Sheinberg DL, Logothetis NK (1997) The role of temporal cortical areas in perceptual organization. Proc. Natl. Acad. Sci. USA 94: 3408–3413.

Walker P (1975) Stochastic properties of binocular rivalry. Percept Psychophys. 18: 467–473.

Walker P (1976) The perceptual fragmentation of unstabilized images. Q. J. Exp. Psychol. 28: 35–45.

Wang XJ (1999) Synaptic basis of cortical persistent activity: The importance of NMDA receptors to working memory. J. Neurosci. 19(21): 9587–9603.

Wilson HR, Blake R, Lee SH (2001) Dynamics of travelling waves in visual perception. Nature 412: 907–910.

Wilson HR, Krupa B, Wilkinson F (2000) Dynamics of perceptual oscillations in form vision. Nat. Neurosci. 3(2): 170–176.